Published in final edited form as:
Bipolar Disord. 2013 September ; 15(6): 680–693. doi:10.1111/bdi.12096.

Overlapping and Distinct Gray and White Matter Abnormalities in Schizophrenia and Bipolar I Disorder

Dana Anderson[1,2,*], **Babak A. Ardekani**[3,*], **Katherine E. Burdick**[4], **Delbert G. Robinson**[1,2,5], **Majnu John**[1,2], **Anil K. Malhotra**[1,2,5], and **Philip R. Szeszko**[1,2,5]

[1]The Feinstein Institute for Medical Research, North Shore-LIJ Health System, Manhasset, NY

[2]The Zucker Hillside Hospital, North Shore-LIJ Health System, Glen Oaks, NY

[3]The Nathan S. Kline Institute for Psychiatric Research, Orangeburg, NY

[4]Departments of Psychiatry and Neuroscience, Mount Sinai School of Medicine, NY, NY

[5]Hofstra North Shore – LIJ School of Medicine, Departments of Psychiatry and Molecular Medicine, Hempstead, NY, USA

Abstract

Background—Schizophrenia and bipolar disorder may share common neurobiological mechanisms, but few studies have directly compared gray and white matter structure in these disorders. We used diffusion-weighted magnetic resonance imaging and a region-of-interest based analysis to identify overlapping and distinct gray and white matter abnormalities in 35 patients with schizophrenia and 20 patients with bipolar I disorder in comparison to 56 healthy volunteers.

Methods—We examined fractional anisotropy within the white matter and mean diffusivity within the gray matter in 42 regions-of-interest defined on a probabilistic atlas following non-linear registration of the images to atlas space.

Results—Patients with schizophrenia had significantly lower fractional anisotropy in temporal (superior temporal and parahippocampal) and occipital (superior and middle occipital) white matter compared to patients with bipolar disorder and healthy volunteers. In contrast, both patient groups demonstrated significantly higher mean diffusivity in frontal (inferior frontal and lateral orbitofrontal) and temporal (superior temporal and parahippocampal) gray matter compared to healthy volunteers, but did not differ from each other.

Discussion—Our study implicates overlapping gray matter frontal and temporal lobe structural alterations in the neurobiology of schizophrenia and bipolar I disorder, but suggests that temporal and occipital lobe white matter deficits may be an additional risk factor for schizophrenia. Our findings may have relevance for future diagnostic classification systems and the identification of susceptibility genes for these disorders.

INTRODUCTION

A dichotomy between schizophrenia and bipolar disorder was originally described by Kraepelin (1) and continues today in the nosological classes of schizophrenia and bipolar disorder as defined operationally in the DSM-IV (2). It is increasingly recognized, however,

Author correspondence: Philip R. Szeszko, Ph.D., The Zucker Hillside Hospital, Psychiatry Research, 75-59 263rd Street, Glen Oaks, NY 11004; Phone: (718) 470-8489; Fax: (718) 343-1659; szeszko@lij.edu.
*These authors contributed equally to this work

Conflicts of Interest
The authors affirm that there are no conflicts of interest that may have influenced this work.

that schizophrenia and bipolar disorder share certain epidemiological features such as age at onset (3), genetic risk (4), incidence (5) and influence of sex (6, 7). Moreover, the estimated lifetime risk of bipolar disorder in first-degree relatives of bipolar patients is 40–70% in monozygotic twins (8), which is similar compared to the 50% risk estimate for monozygotic twins for schizophrenia (9). Along these lines there is converging evidence from genetics studies supporting the hypothesis that bipolar disorder and schizophrenia may share common endophenotypes (10) and genes including Disrupted in Schizophrenia 1 (11, 12), dystrobrevin binding protein 1 (DTNBP1) (13), neuregulin 1 (14–15), catechol-*o*-methyl transferase (16), and G72 [D-amino acid oxidase activator, (DAOA)]/G30 loci (17, 18). In addition, recent genome-wide association data have confirmed several convincing risk loci for schizophrenia (19) and bipolar disorder (20). Consistent with the family-based evidence of considerable genetic overlap (4), many of the variants initially identified as predisposing to SZ have subsequently been associated with BPD, and vice versa. A recent cross-phenotype study reported that 6 of the 8 SNPs most robustly associated with either SZ or BPD show *trans*-disorder effects (21), including CACNA1C (alpha-1C subunit of the L-type voltage-gated calcium channel) (22–25).

Magnetic resonance (MR) imaging has provided important information regarding the potential overlap of structural abnormalities in patients with bipolar disorder and schizophrenia. Several studies reported less gray matter in the thalamic region (26–27), and medial frontal gyrus (28) in both disorders compared to healthy volunteers. Other studies, however, indicated that compared to patients with bipolar disorder, schizophrenia is characterized by widely distributed gray matter deficits predominantly involving the fronto-temporal neocortex (29; 30), hippocampus (31,32; 33), cerebellum (34), thalamus (34), Heschl's gyrus (35) and left planum temporale (35). In contrast, compared to schizophrenia, patients with bipolar disorder reportedly have gray matter deficits in regions that have been strongly implicated in emotional processing including the anterior cingulate gyrus (36), and the amygdala (31, 32).

Diffusion tensor imaging (DTI) is an *in-vivo* MR imaging approach that can be used to examine white matter and gray matter integrity in humans. Mean diffusivity (MD) and fractional anisotropy (FA) are scalar-valued measures that can be computed from the estimated diffusion tensor (DT) and reflect the magnitude and anisotropy of the self-diffusion of water molecules in the brain, respectively. FA is a non-linear function of the 3 eigenvalues of the DT that varies between 0 and 1. It provides information regarding the shape of the DT and is typically used as an index of white matter integrity (37, 38). Little work has directly compared FA in patients with schizophrenia to those with bipolar disorder. In two prior studies, however, lower FA was observed in both patient groups compared to healthy volunteers in the white matter comprising the uncinate fasciculus and anterior thalamic radiation (39, 40).

MD is the average of the three diagonal elements of the DT or equivalently the average of its three eigenvalues. In contrast to FA, MD quantifies the magnitude of water diffusion within tissues (41) as opposed to the directional preference of diffusion. Unlike diffusion anisotropy measures, which are higher in coherent white matter, MD is greater in cerebral spinal fluid (CSF) where water diffusion is not restricted by cellular fibers and structure (42). In gray matter, increased MD is likely due to the effect of increased unoccupied intercellular space and not due to a change in neuronal cell density, thus, it may be the result of lower cortical neuropil, which includes axonal, dendritic, and glial braches (43). MD has been utilized to assess gray matter integrity in patients with schizophrenia compared to healthy controls (e.g., 43–46) and may be a sensitive marker for the detection of early structural abnormalities in first-episode schizophrenia (46). Notably, MD has also been used

to assess gray matter integrity in other disorders including multiple sclerosis (47), dementia (48, 49), Parkinson's disease (50) and major depression (51).

Few studies have examined overlapping and distinct patterns of both gray and white matter in patients with schizophrenia or bipolar disorder compared to each other and healthy volunteers. Moreover, unlike prior studies that used diffusion tensor imaging to investigate white matter structure, we used segmented regions-of-interest to investigate FA within the white matter and MD within the gray matter, respectively as defined on a probabilistic atlas following non-linear registration of the diffusion tensor imaging data to atlas space. We hypothesized that gray and white matter abnormalities would be evident in frontal and temporal lobe regions among patients with schizophrenia and bipolar disorder compared to healthy volunteers consistent with previously published structural and diffusion tensor imaging studies (e.g., 36, 52).

METHODS

Subjects

Fifty-five patients with a diagnosis of schizophrenia or bipolar I disorder were recruited from the Zucker Hillside Hospital in Glen Oaks, NY. Diagnoses were based on clinical interview using the SCID for DSM-IV Disorders (53) and supplemented by medical records and information provided by clinicians and family members, when available. Subtypes for the 35 patients with schizophrenia included disorganized (N=1), paranoid (N=18) and undifferentiated (N=16). Twenty patients with a diagnosis of bipolar disorder I disorder were included and all but 2 had a history of psychosis during acute episodes. Patients were being treated with antipsychotic medications (n=32), mood stabilizers (N=6) or both antipsychotics and mood stabilizers (N=12). Two patients were not receiving psychotropic medications and medication data were unavailable for 3 patients. Fifty-six healthy volunteers were recruited from the community to match the patient groups in distributions of age and sex. Exclusion criteria for healthy subjects included any history of Axis I psychiatric illness as assessed by clinical interview (SCID-NP) (54). In addition, exclusion criteria for all study participants included any serious medical or neurological condition known to affect the brain and MR imaging contraindications. This study was approved by the North Shore-Long Island Jewish Medical Center Institutional Review Board and written informed consent was obtained from all study participants.

Handedness

Handedness was assessed for subjects using a modified 20-item version of the Edinburgh Inventory. A laterality quotient was computed for all individuals using the following formula: (Total R − Total L)/(Total R + Total L), where "Total R" and "Total L" refer to the total number of right and left hand items scored, respectively. Scores thus ranged from 1.0 (totally dextral) to −1.0 (totally non-dextral). Individuals with laterality scores greater than . 7 were classified as dextral and the remaining subjects were classified as non-dextral. Handedness for 9 individuals was based on preference for handwriting alone.

Magnetic Resonance (MR) Imaging Procedures

All MR imaging scans were acquired at the Long Island Jewish Medical Center using a 1.5T GE system and were reviewed clinically by a radiologist with none demonstrating gross pathology. We acquired 26 DTI volumes from each subject, which included 25 volumes with diffusion gradients applied along 25 non-parallel directions with b = 1000 s/mm^2 and NEX = 2, and one volume without diffusion weighting (b = 0; NEX = 2). Each volume consisted of 23 contiguous 5-mm axial slices acquired parallel to the anterior-posterior (AC-PC) commissural line using a ramp sampled, spin-echo, single shot echo-planar imaging

(EPI) method (TR = 10 s, TE = min, FOV = 22 cm, matrix size = 128 x 128). For each subject, the FA and MD maps were computed from the 26 DTI volumes following estimation of a DT matrix at each voxel using a log-linear least squares estimation method. An oblique axial fast spin echo scan (TR = 4 s, TE = 20/100 ms, FOV = 22 cm, matrix size = 256 x 256) was also acquired using the same slice prescription as the DTI and provided contiguous 5-mm thick proton density (PD; TE = 20 ms) and T2-weighted (T2; TE = 100 ms) images. In addition, 124 contiguous coronal images (slice thickness = 1.5 mm) were acquired through the whole head using a 3D Fast SPGR sequence with IR Prep (TR = 10.1 ms, TE = 4.3 ms, TI = 600 ms, FOV = 22 cm, matrix size = 256 x 256).

Probabilistic Atlas

We created a probabilistic atlas in the same space as the Montreal Neurologic Institute's 'Colin27' MR imaging volume (55). The probabilistic atlas was created using the LPBA40 dataset (56) that consists of 40 high-resolution T1-weighted structural brain scans from 40 volunteers, on each of which 56 anatomical structures have been manually labeled (Figure 1). We used '3dwarper', the non-linear registration module of the Automatic Registration Toolbox (ART) (57), to register all 40 MR imaging scans of the LPBA40 dataset to the Colin27 image. We then applied the resulting non-linear transformations to each of the 56 structure label maps of each subject to transform them into the same space as the Colin27 image. Thus, for each of the 56 structures, we obtained 40 label maps in standard space. These label maps were averaged to create the probabilistic atlas that we refer to as the LPBA40/ART atlas (Figure 1). Using the LPBA40/ART atlas, it is possible to automatically determine a given structure on any test image after co-registration of the test image with the Colin27 brain. By inverting the transformation and applying it to the LPBA40/ART atlas, it is possible to project the atlas labels on the space of the test image, thus automatically delineating the 56 structures onto the test image. The LPBA40 data set also includes automatically segmented gray matter (GM), white matter (WM), and cerebrospinal fluid (CSF) labels for each of the 40 cases. These were also transformed to the Colin27 space and averaged to yield tissue-type probabilistic labels. Thus, the probabilistic atlas that was created included label maps for the 56 structures as well as GM, WM, and CSF in the reference space of the Colin27 brain.

Image Registration

The purpose of image registration was to find a non-linear transformation that registers the FA and MD maps derived from the DTI data to the Colin27 brain. When such a transformation is found, it can then be inverted and applied to the LPBA40/ART atlas, which then automatically propagates the structure and tissue-type labels of the atlas onto the space of the FA or MD map. This permits ROI analysis of the average FA and MD values on the 56 structures as a whole, or on specific tissue types (e.g., GM, WM, or CSF) within each structure. Image registration was conducted using methods published previously (58, 59) and are described briefly. Non-brain regions were initially removed from the SPGR image using the Brain Extraction Tool (BET) (60) with any remaining tissue removed manually using MEDx (Sensor Systems, Inc., MD, USA). We next normalized the skull-stripped SPGR (SS-SPGR) image to the Colin27 MR imaging volume using 3dwarper in ART. In addition, we employed a rigid-body 6-parameter linear transformation (61) to register the SS-SPGR image to the fast spin echo T2 volume. Using this transformation, the SS-SPGR was re-sliced to match the T2 volume and subsequently used to skull-strip the T2 volume. To correct for spatial distortion in the DTI EPI images, the b=0 DTI volume was non-linearly registered to the skull-stripped T2 (SS-T2) volume using ART. Lastly, we combined the transformations obtained from each of the three registration steps (i.e., DTI-to-T2; T2-to-SPGR; SPGR-to-Colin27) to obtain a single transformation (DTI-to-Colin27) that would register the FA or MD images to the stereotactic space of the Colin27 template.

Region-of-Interest Analyses

The aim of the region-of-interest (ROI) analysis was to determine average FA and MD values in apriori defined brain regions on the LPBA40/ART atlas. For each subject, we registered the FA and MD maps to the LPBA40/ART atlas space (Colin27 brain template space) using the methods described above. We then applied the inverse of the resulting non-linear transformation to the LPBA40/ART atlas to propagate the regional and tissue-type atlas labels onto the FA and MD maps in the native space. Average FA and MD values in these ROIs were then computed as follows. We let m_j represent the FA (or MD) value at voxel j, and p_{ij} represent the probabilistic ROI information obtained from the LPBA40/ART atlas at voxel j for regions i=1, 2, …, n. In particular, p_{ij} represented the probability that voxel j belongs to region i. The average FA or MD in a given region i was thus computed as follows:

$$\overline{m_i} = \frac{\sum_j p_{ij} m_j}{\sum_j p_{ij}}$$

In this study, we analyzed average FA and MD values for 21 ROIs in the right and left hemispheres: superior frontal gyrus, middle frontal gyrus, inferior frontal gyrus, precentral gyrus, middle orbitofrontal gyrus, lateral orbitofrontal gyrus, superior temporal gyrus, middle temporal gyrus, inferior temporal gyrus, parahippocampal gyrus, postcentral gyrus, superior parietal gyrus, supramarginal gyrus, angular gyrus, precuneus, superior occipital gyrus, middle occipital gyrus, inferior occipital gyrus, fusiform gyrus, cingulate gyrus and hippocampus.

As noted, the LPBA40/ART atlas also includes probabilistic tissue type information. Projected in native space, this information may be represented by three probabilistic maps: $\{p_{wmj}\}$, $\{p_{gmj}\}$, and $\{p_{csfj}\}$, where, for example, p_{gmj}, represents the probability that voxel j belongs to tissue-type: gm (gray matter). The tissue probability maps were combined with the 42 aforementioned region probability maps to obtain 3x42 maps $\{p_{wmij}\}$, $\{p_{gmij}\}$, and $\{p_{csfij}\}$ where each of the regions were divided into GM, WM and CSF. Combining the tissue-type probability maps and the region probability maps was accomplished by using a threshold T to define: $p_{gmij} = p_{ij}$ if $p_{gmij} > T$; and $p_{gmij}=0$ otherwise. We used the threshold level of 30% for gray matter and 70% for white matter to obtain tissue-type specific averages for each of the regions. Thus, we were able to obtain tissue-specific average FA (or MD) values. For example, the average gray matter MD in region i was computed as follows:

$$\overline{m_{gmi}} = \frac{\sum_j p_{gmij} m_j}{\sum_j p_{gmij}}$$

Statistical Analyses

Categorical variables were compared among groups by chi-square tests and continuous measures were analyzed using one way ANOVA. Outlying values for FA and MD (defined as 3 standard deviations from the mean) were replaced with values 3 SD below or above the sample mean. Given the lack of robust group-by-hemisphere interactions both right and left hemisphere regions were averaged for analyses to increase power and limit Type-I error. To further limit Type-I error we averaged individual brain structures from the LPBA40 Atlas to form 5 brain lobules. These included: (1) “frontal” consisting of superior frontal gyrus, middle frontal gyrus, inferior frontal gyrus, precentral gyrus, middle orbitofrontal gyrus, and lateral orbitofrontal gyrus; (2) “temporal” consisting of superior temporal gyrus, middle temporal gyrus, inferior temporal gyrus, parahippocampal gyrus and fusiform gyrus; (3)

"parietal" consisting of postcentral gyrus, superior parietal gyrus, supramarginal gyrus, angular gyrus, and precuneus; (4) "occipital" consisting of superior occipital gyrus, middle occipital gyrus and inferior occipital gyrus and (5) "limbic" consisting of cingulate gyrus and hippocampus.

Repeated measures ANCOVA (SPSS for Windows, version 11.5; SPSS, Chicago, IL) was used to compare brain structure volumes among the patient groups and healthy volunteers with alpha set to .05 (two-tailed). FA was examined within the white matter and MD within the gray matter in separate analyses. In each analysis the between subjects factors included group (patients with schizophrenia versus patients with bipolar disorder versus healthy volunteers) and sex and the within subjects factor included lobule (frontal, temporal, parietal, occipital and limbic). Greenhouse-Geisser correction was used in each analysis given that Mauchly's test of Sphericity was significant. Age was included as a statistical covariate given that it correlated with FA and MD. We specifically were interested in testing group-by-region interactions in analyses of FA and MD, which, if significant, were followed by univariate ANCOVAs for each of the 5 brain lobules to test for group main effects. Any significant group main effect was subsequently followed by ANCOVAs examining group differences within each individual brain region comprising the lobule. In addition to these primary analyses we conducted univariate ANCOVAs among groups for every individual brain region (with age as a covariate) for descriptive purposes (Tables 2 and 3) where effect size measures are presented as partial eta-squared.

Results

The groups did not differ significantly from one another in distributions of race, sex, age, handedness, years of education, and age at onset (Table 1). Mean FA and MD values along with the adjusted 95% confidence intervals for the difference between group means are provided for all of the individual brain regions in Tables 2 and 3, respectively, for descriptive purposes only.

In FA analyses the main finding that distinguished the groups was a significant group-by-region interaction ($F = 3.87$, $df = 6.77$, $p = .001$). Followup unvariate ANCOVAs revealed significant main effects of group for the temporal ($F = 4.36$, $df = 2,104$, $p = 0.015$) and occipital ($F = 8.70$, $df = 2,104$, $p < .001$) lobes. Posthoc analyses of individual regions indicated that patients with schizophrenia had significantly lower FA compared to patients with bipolar disorder and healthy volunteers in the superior temporal ($F = 5.85$, $df = 2,104$, $p = 0.004$), parahippocampal ($F = 5.28$, $df = 2,104$, $p = 0.007$), superior occipital ($F = 5.78$, $df = 2,104$, $p = 0.004$) and middle occipital ($F = 10.02$, $df = 2,104$, $p < 0.001$) white matter.

In the MD analyses there also was a significant group-by-region interaction ($F = 2.31$, $df = 6.39$, $p = .03$); significant main effects of group were evident in the frontal ($F = 5.07$, $df = 2, 104$, $p = .008$), parietal ($F = 3.99$, $df = 2, 104$, $p = .021$), limbic ($F = 5.71$, $df = 2, 104$, $p = .004$), and temporal ($F = 8.26$, $df = 2, 104$, $p < 0.001$) lobe regions. Posthoc analyses of individual regions indicated that both patient groups had significantly higher MD in the superior temporal ($F = 7.39$, $df = 2, 104$, $p = 0.001$), parahippocampal ($F = 7.08$, $df = 2, 104$, $p = 0.001$), fusiform ($F = 4.30$, $df = 2, 104$, $p = .016$), angular ($F = 4.90$, $df = 2, 104$, $p = .009$), supramarginal ($F = 5.26$, $df = 2, 104$, $p = .007$), lateral orbital frontal ($F = 5.62$, $df = 2, 104$, $p = .005$) and inferior frontal ($F = 6.85$, $df = 2, 104$, $p = .002$) regions compared to healthy controls, but that the patient groups did not differ from each other. In addition, patients with bipolar disorder had significantly higher MD in the postcentral ($F = 5.55$, $df = 2, 104$, $p = .005$) region compared to healthy controls and higher MD in the precentral ($F = 5.52$, $df = 2, 104$, $p = .005$) and middle frontal ($F = 3.95$, $df = 2, 104$, $p = .022$) regions compared both to healthy volunteers and patients with schizophrenia. Moreover, patients

with schizophrenia had higher MD in the middle temporal ($F = 4.26$, $df = 2, 104$, $p = .017$) and hippocampal ($F = 6.76$, $df = 2, 104$, $p = .002$) regions compared to healthy volunteers and higher MD in the inferior temporal ($F = 6.68$, $df = 2, 104$, $p = .002$) region compared both to healthy volunteers and patients with bipolar disorder.

Age and Sex Effects

There was a significant ($F = 16.86$, $df = 1, 104$, $p < .001$) main effect of sex for FA with males having higher FA compared to females across all brain regions. The region-by-age interaction was statistically significant ($F = 3.11$, $df = 3.39$, $p = .022$) for FA with posthoc analyses indicating that age correlated inversely with FA across groups in the frontal lobes ($F = 8.74$, $df = 2,104$, $p = .004$). The region-by-age interaction was statistically significant for MD ($F = 7.02$, $df = 3.19$, $p < .001$) with posthoc analyses indicating that age correlated positively with MD across groups in the frontal ($F = 20.05$, $df = 2, 104$, $p < 0.001$), limbic ($F = 5.71$, $df = 2, 104$, $p = .016$), parietal ($F = 18.60$, $df = 2, 104$, $p < 0.001$), temporal ($F = 5.54$, $df = 2, 104$, $p = .02$) and occipital ($F = 10.65$, $df = 2, 104$, $p = 0.001$) lobes. No significant main effect of sex was evident in the analysis of MD. The region-by-sex and region-by-group-by-sex interactions were not statistically significant in either the FA or MD analyses.

DISCUSSION

Understanding the unique contributions of gray and white matter abnormalities in schizophrenia and bipolar disorder as well as their potential overlap can inform neurobiological models of these disorders and diagnostic classification systems. In contrast to prior work that used diffusion tensor imaging to only investigate the white matter, we employed segmented gyri as regions-of-interest defined a priori to investigate FA within the white matter and MD within the gray matter. A potential advantage of using MD as a surrogate marker of gray matter volume deficits compared to voxel-based approaches is that it may be more sensitive to volume changes. The main findings of our study indicate that schizophrenia is characterized by white matter abnormalities in temporal and occipital regions compared both to patients with bipolar disorder and healthy volunteers. In contrast to the pattern of white matter findings, gray matter structural alterations appeared generally comparable in frontal and temporal lobe regions between patients with bipolar disorder and schizophrenia, but abnormal in these two patient groups compared to healthy volunteers. Our data are consistent with the hypothesis that these disorders share overlapping gray matter structural deficits, but that schizophrenia may additionally involve aberrant white matter integrity in temporal and occipital regions.

Few studies have assessed white matter integrity in both schizophrenia and bipolar disorder and thus, it is difficult to directly compare our results to prior findings. Two studies reported comparable white matter abnormalities between patients with bipolar disorder and those with schizophrenia in the anterior limb of the internal capsule, uncinate fasciculus, and anterior thalamic radiations, which in turn were abnormal compared to controls (39, 40). Our data suggest, however, that white matter abnormalities in temporal and occipital lobe regions may be important in differentiating between patients with schizophrenia and those with bipolar disorder. Abnormal white matter has been hypothesized to may play a critical role in the pathophysiology of schizophrenia (62) and several studies have implicated white matter disruptions in the earliest phase of illness (59,63). Abnormal FA observed within the white matter of patients with schizophrenia is consistent with prior work implicating deficits in oligodendrocytes and myelin-related abnormalities in protein and gene expression (64–67) as well as in-vivo neuroimaging studies (68, 69).

It is particularly noteworthy that white matter abnormalities were evident within the superior temporal gyrus in patients with schizophrenia compared to patients with bipolar disorder and healthy volunteers. Our data thus converge with several prior neuroimaging studies implicating white matter abnormalities in this region in patients with schizophrenia compared to healthy volunteers (59, 63, 70, 71) as well as deficits in regions adjacent to the superior temporal gyrus (71–73). Moreover, magnetization transfer imaging (74), cytoarchitectural (75) and voxel-based morphometry (76–78) studies have also demonstrated superior temporal gyrus white matter abnormalities in patients with schizophrenia. In terms of diagnostic specificity our findings also converge with Beasley et al. (75) who reported that glial cell density was decreased in the superior temporal white matter in schizophrenia compared to controls, but was unchanged in bipolar disorder or the major depressive disorder groups. Moreover, a defect in temporal lobe white matter may play a role in abnormal neuropsychological functioning and positive symptom severity in schizophrenia (59).

Our data also highlight a role for occipital white matter abnormalities in the pathogenesis of schizophrenia compared to patients with bipolar disorder and healthy volunteers. Thus, our results are consistent with prior work implicating white matter abnormalities in the uncinate fasciculus/inferior fronto-occipital fasciculus (79–81), inferior longitudinal fasciculus (79), superior longitudinal fasciculus (80), and occipital lobe (82–84) in patients with schizophrenia compared to healthy volunteers. In addition, in a combined MR imaging and DTI study, patients with first-episode schizophrenia had lower white matter volume in the temporal-occipital region, decreased planar anisotropy and higher linear anisotropy in the right temporal-occipital region compared to healthy volunteers (85). In a study of early-onset schizophrenia patients lower fractional anisotropy was reported in the occipital white matter (86). Although several DTI studies noted occipital lobe white matter abnormalities in bipolar patients compared to healthy volunteers (87–91), little research has compared the magnitude and location of occipital lobe white matter impairment directly between these two disorders. For example, the lack of robust occipital lobe white matter abnormalities among bipolar patients may be related to the fact that several prior findings were observed in the deep and periventricular white matter (58, 93, 94), which were not reflected in our regions-of-interest.

Our study provides evidence for comparable temporal lobe gray matter structural alterations in schizophrenia and bipolar I disorder. Specifically, both groups demonstrated greater MD in superior temporal and parahippocampal gray matter compared to healthy volunteers, but did not differ from each other. Our findings generally converge with a meta-analysis by Ellison-Wright and Bullmore (36) who reported that gray matter abnormalities in schizophrenia overlapped substantially with those in bipolar disorder. More specifically, however, several studies implicated gray matter structural alterations in the parahippocampal gyrus in schizophrenia (95, 96) and bipolar disorder (97, 98). Moreover, although gray matter deficits in the superior temporal gyrus have been well-replicated in schizophrenia compared to healthy controls (e.g., 99, 100), they have also been reported in bipolar disorder (101,102). Given that the majority of bipolar patients in our study had a history of psychotic features it is conceivable that gray matter structural deficits in the superior temporal gyrus and parahippocampal gyrus might reflect a common neurobiological substrate related to psychosis. For example, compared to healthy controls, recent-onset (103) and first-episode (104) psychotic patients demonstrated temporal gray matter deficits. Similarly, both schizophrenia and bipolar patients with mood-incongruent psychotic symptoms in the form of persecutory delusions had temporal lobe gray matter deficits (105).

Recent literature reviews indicate robust evidence for frontal lobe structural alterations both in schizophrenia (106) and bipolar disorder (107), but few studies have directly compared

the magnitude of these deficits in both disorders. In a recent meta-analysis Yu et al (108) reported substantial overlap in prefrontal gray matter regions in schizophrenia and bipolar disorder with several reports implicating gray matter deficits in the orbital frontal gyri and inferior frontal gyri in schizophrenia (109–112) and bipolar disorder (113, 114) compared to healthy volunteers. Our findings thus converge with prior studies implicating comparable frontal gray matter structural alterations in both patient groups compared to healthy volunteers. Abnormalities in the orbital frontal and inferior frontal regions may contribute to neuropsychological deficits in olfaction (115) and go no/go performance (116, 117) observed in both patients with schizophrenia and bipolar disorder.

There were several study limitations that should be acknowledged. The sample sizes were modest, although the patient groups were well-characterized diagnostically, which may have decreased subject variability and increased our ability to detect group differences. On the other hand, it is conceivable that structural alterations in these disorders might be evident in other regions if larger subject groups were investigated. Patients were also receiving antipsychotic medications and/or mood stabilizers and thus, the potential influence of these medications on the dependent measures may limit study interpretation. It should be acknowledged that clinical and neuropsychological measures were unavailable for patients, and thus we did not clarify the functional sequelae of these patient differences. Also, a potential downside of using diffusion weighted imaging for assessing gray matter integrity is that the results are not easily quantifiable. Moreover, given that we did not perform tractography we did not have information available regarding the specific tracts affected in the FA analysis of the white matter. Our use of an atlas (118), however, suggested that the superior temporal white matter likely included the inferior longitudinal fasciculus and uncinate fasciculus whereas the parahippocampal region included part of the cingulum bundle. In addition, the superior and middle occipital white matter regions likely encompassed the inferior fronto-occipital fasciculus and corona radiata.

In summary, the results of the present study support the hypothesis that schizophrenia and bipolar disorder are characterized by comparable gray matter structural alterations, but that white matter disruptions in temporal and occipital regions may pose an additional risk factor for schizophrenia. Additional neuroimaging studies with larger sample sizes and the use of combined genetic/neuroimaging paradigms may further elucidate both the shared and distinct gray and white matter differences that play a role in the etiology of these disorders.

Acknowledgments

This work was supported in part by grants from NARSAD (PRS) and the National Institute of Mental Health to Dr. Szeszko (MH76995), Dr. Robinson (MH60004), the NSLIJ Research Institute General Clinical Research Center (M01 RR18535), an Advanced Center for Intervention and Services Research (MH74543) and a Center for Intervention Development and Applied Research (MH80173)

References

1. Diefendorf, AR., translator and editor. Kraepelin E Clinical psychiatry: A text-book for students and physicians. 6. New York & London: Macmillan; 1902. Original work published in 1899 as Psychiatrie
2. Craddock N, O'Donovan MC, Owen MJ. Genes for schizophrenia and bipolar disorder? Implications for psychiatric nosology. Schizophr Bull. 2006; 32:9–16. [PubMed: 16319375]
3. Ongur D, Lin L, Cohen BM. Clinical characteristics influencing age at onset in psychotic disorders. Compr Psychiatry. 2009; 50:13–19. [PubMed: 19059508]
4. Lichtenstein P, Yip BH, Bjork C, et al. Common genetic determinants of schizophrenia and bipolar disorder in Swedish families: A population-based study. Lancet. 2009; 373:234–239. [PubMed: 19150704]

5. Herrell R, Henter ID, Mojtabai R, et al. First psychiatric hospitalizations in the U.S military: The National Collaborative Study of Early Psychosis and Suicide (NCSEPS). Psychol Med. 2006; 36:1405–1415. [PubMed: 16879759]
6. Laursen TM, Munk-Olsen T, Nordentoft M, et al. A comparison of selected risk factors for unipolar depressive disorder, bipolar affective disorder, schizoaffective disorder, and schizophrenia from a Danish population-based cohort. J Clin Psychiatr. 2007; 68:1673–1681.
7. Welham JL, Thomis R, McGrath JJ. Age-at-first-registration and heterogeneity in affective psychoses. Aust N Z J Psychiatr. 2003; 37:66–69.
8. Moller H. Bipolar disorder and schizophrenia: Distinct illnesses or a continuum? J Clin Psychiatr. 2003; 64(Suppl 6):23–27.
9. Tsuang M, Stone WS, Faraone SV. Genes, environment and schizophrenia. The British J of Psychiat. 2001; 178:s18–s24.
10. Thaker GK. Neurophysiological endophenotypes across bipolar and schizophrenia psychosis. Schizophr Bull. 2008; 34:760–763. [PubMed: 18502737]
11. Hodgkinson CA, Goldman D, Jaeger J, et al. Disrupted in schizophrenia 1 (DISC1): Association with schizophrenia, schizoaffective disorder, and bipolar disorder. Am J Hum Genet. 2004; 75:862–872. [PubMed: 15386212]
12. Maeda K, Nwulia E, Chang J, et al. Differential expression of disrupted-in-schizophrenia (DISC1) in bipolar disorder. Biol Psychiatry. 2006; 360:929–935. [PubMed: 16814263]
13. Gaysina D, Cohen-Woods S, Chow PC, et al. Association of the dystrobrevin binding protein 1 gene (DTNBP1) in a bipolar case-control study (BACCS). Am J Med Genet Part B, Neuropsychiatr Genet. 2009; 150B:836–844.
14. Georgieva L, Dimitrova A, Ivanov D, et al. Support for neuregulin 1 as a susceptibility gene for bipolar disorder and schizophrenia. Biol Psychiatry. 2008; 64:419–427. [PubMed: 18466881]
15. Prata DP, Breen G, Osborne S, et al. An association study of the neuregulin 1 gene, bipolar affective disorder and psychosis. Psychiatr Genet. 2009; 29:113–116. [PubMed: 19339916]
16. Shifman S, Bronstein M, Sternfeld M, et al. A. COMT: A common susceptibility gene in bipolar disorder and schizophrenia. Am J Med Genet Part B, Neuropsychiatr Genet. 2004; 128B:61–64.
17. Hattori E, Liu C, Badner JA, et al. Polymorphisms at the g72/g30 gene locus, on 13q33, are associated with bipolar disorder in two independent pedigree series. Am J Hum Genet. 2003; 72:1131–1140. [PubMed: 12647258]
18. Detera-Wadleigh SD, McMahon FJ. G72/G30 in schizophrenia and bipolar disorder. Biol Psychiatry. 2006; 60:106–114. [PubMed: 16581030]
19. Ripke S, Sanders AR, Kendler KS, et al. Schizophrenia Psychiatric Genome-Wide Association Study (GWAS) Consortium. Genome-wide association study identifies five new schizophrenia loci. Nat Genet. 2011; 43(10):969–76. [PubMed: 21926974]
20. Sklar P, Ripke S, Scott LJ, et al. Large-scale genome-wide association analysis of bipolar disorder identifies a new susceptibility locus near ODZ4. Nat Genet. 2011; 43(10):977–83. [PubMed: 21926972]
21. Williams HJ, Craddock N, Russo G, et al. Most genome-wide significant susceptibility loci for schizophrenia and bipolar disorder reported to date cross-traditional diagnostic boundaries. Hum Mol Genet. 2011; 20(2):387–91. [PubMed: 21037240]
22. Green EK, Grozeva D, Jones I, et al. The bipolar disorder risk allele at CACNA1C also confers risk of recurrent major depression and of schizophrenia. Mol Psychiatry. 2010; 15(10):1016–22. [PubMed: 19621016]
23. Sklar P, Smoller JW, Fan J, et al. Whole-genome association study of bipolar disorder. Mol Psychiatry. 2008; 13(6):558–69. [PubMed: 18317468]
24. Ferreira MA, O'Donovan MC, Meng YA, et al. Collaborative genome-wide association analysis supports a role for ANK3 and CACNA1C in bipolar disorder. Nat Genet. 2008; 40(9):1056–8. [PubMed: 18711365]
25. Nyegaard M, Demontis D, Foldager L, et al. CACNA1C (rs1006737) is associated with schizophrenia. Mol Psychiatry. 2010; 15(2):119–21. [PubMed: 20098439]

26. McIntosh AM, Job DE, Moorhead TW, et al. Voxel-based morphometry of patients with schizophrenia or bipolar disorder and their unaffected relatives. Biol Psychiatry. 2004; 56:544–552. [PubMed: 15476683]
27. Yu K, Cheung C, Leung M, Li Q, Chua S, McAlonan G. Are Bipolar Disorder and Schizophrenia Neuroanatomically Distinct? An Anatomical Likelihood Meta-analysis. Front Hum Neurosci. 2010 Oct 26.4:189. [PubMed: 21103008]
28. Janssen J, Reig S, Parellada M, et al. Regional gray matter volume deficits in adolescents with first-episode psychosis. J Am Acad Child Adolesc Psychiatry. 2008; 47:1311–1320. [PubMed: 18827723]
29. McDonald C, Bullmore E, Sham P, et al. Regional volume deviations of brain structure in schizophrenia and psychotic bipolar disorder: Computational morphometry study. Br J Psychiatry. 2005; 186:369–377. [PubMed: 15863740]
30. Yüksel C, McCarthy J, Shinn A, et al. Gray matter volume in schizophrenia and bipolar disorder with psychotic features. Schizophr Res. 2012 Jul; 138(2–3):177–82. Epub 2012 Mar 21. 10.1016/j.schres.2012.03.003 [PubMed: 22445668]
31. Altshuler LL, Bartzokis G, Grieder T, et al. Amygdala enlargement in bipolar disorder and hippocampal reduction in schizophrenia: An MRI study demonstrating neuroanatomic specificity. Arch of Gen Psychiatr. 1998; 55:663–664. [PubMed: 9672058]
32. Altshuler LL, Bartzokis G, Grieder T, et al. An MRI study of temporal lobe structures in men with bipolar disorder or schizophrenia. Biol Psychiatry. 2000; 48:147–162. [PubMed: 10903411]
33. Brown GG, Lee JS, Strigo IA, et al. Voxel-based morphometry of patients with schizophrenia or bipolar I disorder: a matched control study. Psychiatry Res. 2011 Nov 30; 194(2):149–56. Epub 2011 Sep 15. [PubMed: 21924872]
34. Molina V, Galindo G, Cortés B, et al. Different gray matter patterns in chronic schizophrenia and chronic bipolar disorder patients identified using voxel-based morphometry. Eur Arch Psychiatry Clin Neurosci. 2011 Aug; 261(5):313–22. Epub 2010 Dec 28. 10.1007/s00406-010-0183-1 [PubMed: 21188405]
35. Hirayasu Y, McCarley RW, Salisbury DF, et al. Planum temporale and Heschl gyrus volume reduction in schizophrenia: a magnetic resonance imaging study of first-episode patients. Arch Gen Psychiatry. 2000 Jul; 57(7):692–9. [PubMed: 10891040]
36. Ellison-Wright I, Bullmore E. Anatomy of bipolar disorder and schizophrenia: A meta-analysis. Schizophr Res. 2010; 117:1–12. [PubMed: 20071149]
37. Kubicki M, Westin CF, Maier SE, et al. Diffusion tensor imaging and its application to neuropsychiatric disorders. Harv Rev Psychiatry. 2002 Nov-Dec;10(6):324–36. [PubMed: 12485979]
38. Lim KO, Helpern JA. Neuropsychiatric applications of DTI – A review. NMR in Biomed. 2002; 15:587–593.
39. McIntosh AM, Munoz Maniega S, Lymer GK, et al. White matter tractography in bipolar disorder and schizophrenia. Biol Psychiatry. 2008; 64:1088–1092. [PubMed: 18814861]
40. Sussmann JE, Lymer GKS, McKirdy T, et al. White matter abnormalities in bipolar disorder and schizophrenia detected using diffusion tensor magnetic imaging. Bipolar Disord. 2009; 11:11–18. [PubMed: 19133962]
41. Le Bihan D, Mangin JF, Poupon C, et al. Diffusion tensor imaging: Concepts and applications. J Magn Reson Imaging. 2001; 13:534–546. [PubMed: 11276097]
42. Basser PJ, Pierpaoli C. Microstructural and physiological features of tissues elucidated by quantitative-diffusion-tensor MRI. J Magn Reson B. 1996; 111:209–219. [PubMed: 8661285]
43. Lee K, Yoshida T, Kubicki M, et al. Increased diffusivity in superior temporal gyrus in patients with schizophrenia: A diffusion tensor imaging study. Schizophr Res. 2009; 108:33–40. [PubMed: 19135872]
44. Ardekani BA, Bappal A, D'Angelo D, et al. Brain morphometry using diffusion-weighted magnetic resonance imaging: Application to schizophrenia. Neuroreport. 2005; 16:1455–1459. [PubMed: 16110271]

45. Moriya J, Kakeda S, Abe O, et al. Gray and white matter volumetric and diffusion tensor imaging (DTI) analyses in the early stage of first-episode schizophrenia. Schizophr Res. 2010; 116:196–203. [PubMed: 19854618]
46. Narr KL, Hageman N, Woods RP, et al. Mean diffusivity: A biomarker for CSF-related disease and genetic liability effects in schizophrenia. Psychiatry Res. 2009; 171:20–32. [PubMed: 19081707]
47. Oreja-Guevara C, Rovaris M, Iannucci G, et al. Progressive gray matter damage in patients with relapsing-remitting multiple sclerosis: A longitudinal diffusion tensor magnetic resonance imaging study. Arch Neurol. 2005; 62:578–584. [PubMed: 15824256]
48. Kantarci K, Avula R, Senjem ML, et al. Dementia with Lewy bodies and Alzheimer disease: Neurodegenerative patterns characterized by DTI. Neurology. 2010; 74:1814–1821. [PubMed: 20513818]
49. Whitwell JL, Avula R, Sengem ML, et al. Gray and white matter diffusion in the syndromic variants of frontotemporal dementia. Neurology. 2010; 74:1279–1287. [PubMed: 20404309]
50. Kendi ATK, Lehericy S, Luciana M, et al. Altered diffusion in the frontal lobe in Parkinson Disease. Am J Neuroradiol. 2008; 29:501–505. [PubMed: 18202242]
51. Abe O, Yamasue H, Kasai K, et al. Voxel-based analyses of gray/white matter volume and diffusion tensor data in major depression. Psychiatry Res. 2010; 181:64–70. [PubMed: 19959342]
52. Strakowski SM, Delbello MP, Adler CM. The functional neuroanatomy of bipolar disorder: a review of neuroimaging findings. Mol Psychiatry. 2005; 10:105–116. [PubMed: 15340357]
53. First, MB.; Spitzer, RL.; Gibbon, M., et al. Structured Clinical Interview for DSM-IV-TR Axis I Disorders, Research Version, Patient Edition (SCID-I/P). New York: Biometrics Research, New York State Psychiatric Institute; 2002.
54. First, MB.; Spitzer, RL.; Gibbon, M., et al. Structured Clinical Interview for DSM-IV-TR Axis I Disorders, Research Version, Non-patient Edition (SCID-I/NP). New York: Biometrics Research, New York State Psychiatric Institute; 2002.
55. Holmes CJ, Hoge R, Collins L, et al. Enhancement of MR images using registration for signal averaging. J Comput Assist Tomogr. 1998; 22:324–333. [PubMed: 9530404]
56. Shattuck DW, Mirza M, Adisetiyo V, et al. Construction of a 3D probabilistic atlas of human cortical structures. Neuroimage. 2008; 39:1064–1080. [PubMed: 18037310]
57. Ardekani BA, Guckemus S, Bachman A, Hoptman MJ, Wojtaszek M, Nierenberg J. Quantitative comparison of algorithms for inter-subject registration of 3D volumetric brain MRI scans. J Neurosci Methods. 2005 Mar 15; 142(1):67–76. [PubMed: 15652618]
58. Mahon K, Wu J, Malhotra AK, et al. A voxel-based diffusion tensor imaging study of white matter in bipolar disorder. Neuropsychopharmacology. 2009; 34:1590–1600. [PubMed: 19145224]
59. Szeszko PR, Robinson DG, Ashtari M, et al. Clinical and neuropsychological correlates of white matter abnormalities in recent onset schizophrenia. Neuropsychopharmacology. 2008 Apr; 33(5): 976–84. Epub 2007 Jun 20. [PubMed: 17581532]
60. Smith SM. Fast robust automated brain extraction. Hum Brain Mapp. 2002; 17:143–155. [PubMed: 12391568]
61. Ardekani BA, Braun M, Hutton BF, et al. A fully automatic multimodality image registration algorithm. J Comput Assist Tomogr. 1995; 19:615–623. [PubMed: 7622696]
62. Davis KL, Stewart DG, Friedman JI, et al. White Matter Changes in Schizophrenia: Evidence for myelin-related dysfunction. Arch Gen Psychiatr. 2009; 60:443–456. [PubMed: 12742865]
63. Szeszko PR, Ardekani BA, Ashtari M, et al. White matter abnormalities in first-episode schizophrenia or schizoaffective disorder: A diffusion tensor imaging study. Am J Psychiatr. 2005; 162:602–05. [PubMed: 15741480]
64. Flynn SW, Lang DJ, Mackay AL, et al. Abnormalities of myelination in schizophrenia detected in vivo with MRI, and post-mortem with analysis of oligodendrocyte proteins. Mol Psychiatry. 2003; 8:811–820. [PubMed: 12931208]
65. Dracheva S, Davis KL, Chin B, et al. Myelin-associated mRNA and protein expression deficits in the anterior cingulate cortex and hippocampus in elderly schizophrenia patients. Neurobiol Dis. 2006; 21:531–540. [PubMed: 16213148]

66. Katsel P, Davis KL, Haroutunian V. Variations in myelin and oligodendrocyte-related gene expression across multiple brain regions in schizophrenia: A gene ontology study. Schizophr Res. 2005; 79:157–173. [PubMed: 16139990]

67. Tkachev D, Mimmack ML, Ryan MM, et al. Oligodendrocyte dysfunction in schizophrenia and bipolar disorder. Lancet. 2003; 362:798–805. [PubMed: 13678875]

68. Bartzokis G, Nuechterlein KH, Lu PH, et al. Dysregulated brain development in adult men with schizophrenia: A magnetic resonance imaging study. Biol Psychiatry. 2003; 53:412–421. [PubMed: 12614994]

69. Foong J, Symms MR, Barker GJ, et al. Neuropathological abnormalities in schizophrenia: Evidence from magnetization transfer imaging. Brain. 2001; 124:882–892. [PubMed: 11335691]

70. Ardekani B, Nierenberg J, Hoptman MJ, et al. MRI study of white matter diffusion anisotropy in schizophrenia. Neuroreport. 2003; 14:2025–2029. [PubMed: 14600491]

71. Price G, Cercignani M, Chu EM, et al. Brain pathology in first-episode psychosis: Magnetization transfer imaging provides additional information to MRI measurements of volume loss. Neuroimage. 2010; 49:185–192. [PubMed: 19632338]

72. O'Daly OG, Frangou S, Chitnis X, et al. Brain structural changes in schizophrenia patients with persistent hallucinations. Psychiatry Res. 2007; 156:15–21. [PubMed: 17720459]

73. Voineskos AN, Lobaugh NJ, Bouix S, et al. Diffusion tensor tractography findings in schizophrenia across the adult lifespan. Brain. 2010; 133(Pt 5):1494–504. [PubMed: 20237131]

74. Antosik-Biernacka A, Peuskens H, De Hert M, et al. Magnetization transfer imaging in chronic schizophrenia. Med Sci Monit. 2006; 12(4):MT17–MT21. [PubMed: 16572061]

75. Beasley CL, Honavar M, Everall IP, et al. Two-dimensional assessment of cytoarchitecture in the superior temporal white matter in schizophrenia, major depressive disorder and bipolar disorder. Schizophr Res. 2009; 115:156–162. [PubMed: 19833481]

76. Marcelis M, Suckling J, Woodruff P, et al. Searching for a structural endophenotype in psychosis using computational morphometry. Psychiatry Res. 2003; 122:153–167. [PubMed: 12694890]

77. Spalletta G, Tomaiuolo F, Marino V, et al. Chronic schizophrenia as a brain misconnection syndrome: a white matter voxel-based morphometry study. Schizophr Res. 2003; 64:15–23. [PubMed: 14511797]

78. Whitthaus H, Brune M, Kaufmann C, et al. White matter abnormalities in subjects at ultra high-risk for schizophrenia and first-episode schizophrenic patients. Schizophr Res. 2008; 102:141–149. [PubMed: 18515047]

79. Cheung V, Cheung C, McAlonan GM, et al. A diffusion tensor imaging study of structural dysconnectivity in never-medicated, first-episode schizophrenia. Psychol Med. 2008; 38:877–885. [PubMed: 17949516]

80. Koch K, Wagner G, Dahnke R, et al. Disrupted white matter integrity of corticopontine-cerebellar circuitry in schizophrenia. Eur Arch Psychiatr & Clin Neurosci. 2009; 260:419–426.

81. Zhang X, Stein EA, Hong LE. Smoking and schizophrenia independently and additively reduce white matter integrity between striatum and frontal cortex. Biol Psychiatry. 2010; 68:674–677. [PubMed: 20678753]

82. Miyata J, Hirao K, Namiki C, et al. Reduced white matter integrity correlated with cortico-subcortical gray matter deficits in schizophrenia. Schizophr Res. 2009; 111:78–85. [PubMed: 19361957]

83. Tanskanen P, Ridler K, Murray GK, et al. Morphometric brain abnormalities in schizophrenia in a population-based sample: Relationship to duration of illness. Schizophr Bull. 2010; 36:766–777. [PubMed: 19015212]

84. White T, Magnotta VA, Bockholt HJ, et al. Global white matter abnormalities in schizophrenia: A multisite diffusion tensor imaging study. Schizophr Bull. 2011; 37:222–232. [PubMed: 19770491]

85. Chan WY, Yang GL, Chia MY, et al. White matter abnormalities in first-episode schizophrenia: A combined structural MRI and DTI study. Schizophr Res. 2010; 119:52–60. [PubMed: 20056394]

86. Ashtari M, Cottone J, Ardekani BA, et al. Disruption of white matter integrity in the inferior longitudinal fasciculus in adolescents with schizophrenia as revealed by fiber tractography. Arch Gen Psychiatr. 2007; 64:1270–1280. [PubMed: 17984396]

87. Bruno S, Cercignani M, Ron MA. White matter abnormalities in bipolar disorder: a voxel-based diffusion tensor imaging study. Bipolar Disord. 2008; 10:460–468. [PubMed: 18452442]
88. Kafantaris V, Kingsley P, Ardekani B, et al. Lower orbital frontal white matter integrity in adolescents with bipolar I disorder. J Am Acad Child Adolesc Psychiatry. 2009; 48:79–86. [PubMed: 19050654]
89. Macritchie KA, Lloyd AJ, Bastin ME, et al. White matter microstructural abnormalities in euthymic bipolar disorder. Br J Psychiatry. 2010; 196:52–58. [PubMed: 20044661]
90. Regenold WT, D'Agostino CA, Ramesh N, et al. Diffusion-weighted magnetic resonance imaging study of white matter in bipolar disorder: A pilot study. Bipolar Disord. 2006; 8:188–195. [PubMed: 16542190]
91. Wessa M, Houenou J, Leboyer M, et al. Microstructural white matter changes in euthymic bipolar patients: a whole-brain diffusion tensor imaging study. Bipolar Disord. 2009; 11:504–514. [PubMed: 19624389]
92. Zanetti MV, Jackowski MP, Versace A, et al. State-dependent microstructural white matter changes in bipolar I depression. Eur Arch Psychiatry Clin Neurosci. 2009; 259:316–328. [PubMed: 19255710]
93. Monkul ES, Malhi GS, Soares JC. Anatomical MRI abnormalities in bipolar disorder: do they exist and do they progress? Aust N Z J Psychiatr. 2005; 39:222–226.
94. Mahon K, Burdick KE, Szeszko PR. A role for white matter abnormalities in the pathophysiology of bipolar disorder. Neurosci Biobehav Rev. 2010; 34:533–554. [PubMed: 19896972]
95. Glahn DC, Laird AR, Ellison-Wright I, et al. Meta-analysis of gray matter anomalies in schizophrenia: Application of anatomic likelihood estimation and network analysis. Biol Psychiatry. 2008; 64:774–781. [PubMed: 18486104]
96. Yoshihara Y, Sugihara G, Matsumoto H, et al. Voxel-based structural magnetic resonance imaging (MRI) study of patients with early onset schizophrenia. Annals of Gen Psychiatr. 2008; 22:7–25.
97. Almeida JR, Akkal D, Hassel S, et al. Reduced gray matter volume in ventral prefrontal cortex but not amygdala in bipolar disorder: Significant effects of gender and trait anxiety. Psychiatry Res. 2009; 171:54–68. [PubMed: 19101126]
98. Ha TH, Ha K, Kim JH, et al. Regional brain gray matter abnormalities in patients with bipolar II disorder: A comparison study with bipolar I patients and healthy controls. Neurosci Lett. 2009; 456:44–48. [PubMed: 19429131]
99. Takahashi T, Suzuki M, Zhou SY, et al. A follow-up MRI study of the superior temporal subregions in schizotypal disorder and first-episode schizophrenia. Schizophr Res. 2010; 119:65–74. [PubMed: 20051316]
100. Yoshida T, McCarley RW, Nakamura M, et al. A prospective longitudinal volumetric MRI study of superior temporal gyrus gray matter and amygdala-hippocampal complex in chronic schizophrenia. Schizophr Res. 2009; 113:84–94. [PubMed: 19524408]
101. Nugent AC, Milham MP, Bain EE, et al. Cortical abnormalities in bipolar disorder investigated with MRI and voxel-based morphometry. Neuroimage. 2006; 30:485–497. [PubMed: 16256376]
102. Takahashi T, Malhi GS, Wood SJ, et al. Gray matter reduction of the superior temporal gyrus in patients with established bipolar I disorder. J Affect Disord. 2010; 123:276–282. [PubMed: 19766321]
103. Sun D, van Erp TG, Thompson PM, et al. Elucidating a magnetic resonance imaging-based neuroanatomic biomarker for psychosis: Classification analysis using probabilistic brain atlas and machine learning algorithms. Biol Psychiatry. 2009; 66:1055–1060. [PubMed: 19729150]
104. Takahashi T, Wood SJ, Yung AR, et al. Progressive gray matter reduction of the superior temporal gyrus during transition to psychosis. Arch Gen Psychiatr. 2009; 66:366–376. [PubMed: 19349306]
105. Tost H, Ruf M, Schmal C, et al. Prefrontal-temporal gray matter deficits in bipolar disorder patients with persecutory delusions. J Affect Disord. 2010; 120:54–61. [PubMed: 19419772]
106. Shenton ME, Whitford TJ, Kubicki M. Structural neuroimaging in schizophrenia: from methods to insights to treatments. Dialogues Clin Neurosci. 2010; 12:317–322. [PubMed: 20954428]
107. Strakowski SM. Brain structures involved in bipolar disorder: Findings from structural and functional imaging. CNS Spectr. 2007; 12 (6 Suppl 8):5–8. [PubMed: 19317011]

108. Yu K, Cheung C, Leung M, et al. Are bipolar disorder and schizophrenia neuroanatomically distinct? An anatomical likelihood meta-analysis. Front Hum Neurosci. 2010; 4:1–11. [PubMed: 20204154]
109. Buchanan RW, Vladar K, Barta PE, et al. Structural evaluation of the prefrontal cortex in schizophrenia. Am J Psychiatry. 1998; 155:1049–1055. [PubMed: 9699693]
110. Gur RE, Cowell PE, Latshaw A, et al. Reduced dorsal and orbital prefrontal gray matter volumes in schizophrenia. Arch Gen Psychiatr. 2000; 57:761–768. [PubMed: 10920464]
111. Jayakumar PN, Venkatasubramanian G, Gangadhar BN, et al. Optimized voxel-based morphometry of gray matter volume in first-episode, antipsychotic-naive schizophrenia. Prog Neuropsychopharmacol Biol Psychiatry. 2005; 29:587–591. [PubMed: 15866362]
112. Yamasue H, Iwanami A, Hirayasu Y, et al. Localized volume reduction in prefrontal, temporolimbic, and paralimbic regions in schizophrenia: An MRI parcellation study. Psychiatry Res. 2004; 131:195–207. [PubMed: 15465289]
113. Beyer JL, Kuchibhatla M, Payne ME, et al. Gray and white matter brain volumes in older adults with bipolar disorder. Int J Geriatr Psychiatry. 2009; 24:1445–1452. [PubMed: 19452498]
114. Lyoo IK, Kim MJ, Stoll AL, et al. Frontal lobe gray matter density decreases in bipolar I disorder. Biol Psychiatry. 2004; 55:648–651. [PubMed: 15013835]
115. Bitter T, Siegert F, Gudziol H, et al. Gray matter alterations in parosmia. Neuroscience. 2011; 177:177–82. [PubMed: 21241781]
116. Kaladjian A, Jeanningros R, Azorin JM, et al. Reduced brain activation in euthymic bipolar patients during response inhibition: An event-related fMRI study. Psychiatry Res. 2009; 173(1): 45–51. [PubMed: 19442494]
117. Sumich A, Kumari V, Dodd P, et al. N100 and P300 amplitude to Go and No-Go variants of the auditory oddball in siblings discordant for schizophrenia. Schizophr Res. 2008; 98(1–3):265–77. [PubMed: 18022352]
118. Mori, S.; Wakana, S.; van Zijl, PCM.; Nagae-Poetscher, LM., editors. MRI Atlas of Human White Matter. 1. Elsevier Science Hardcover; 2005.

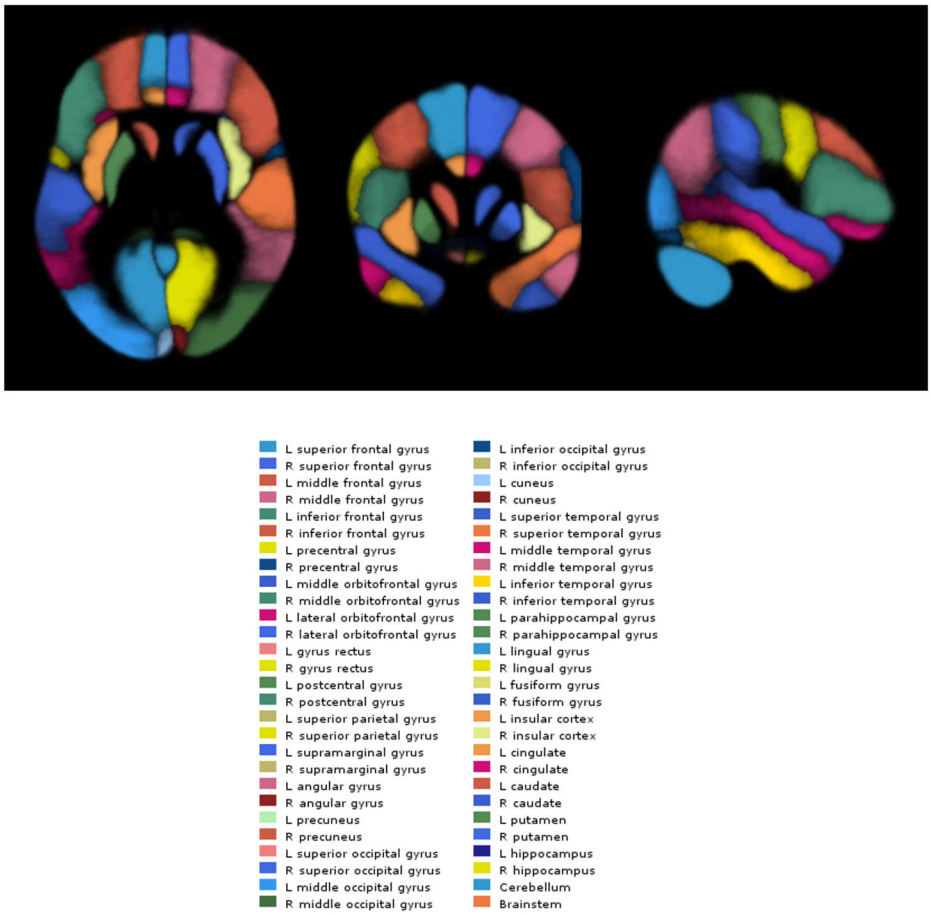

Figure 1.
Illustration of the regions-of-interest from the LPBA40/ART Atlas

Table 1

Sample Characteristics

	Healthy Subjects (n=56)	Patients with Schizophrenia (N=35)	Bipolar I Disorder (N=20)
Sex (M/F)	31/25	23/12	12/8
Age (years)	31.9 (9.4)	30.6 (10.9)	30.7 (6.2)
Handedness (R/L) [a]	49/7	28/6	15/5
Parental Social Class [a,b]	2.5 (1.0)	3.0 (0.95)	2.7 (1.1)
Age at Onset (years)	--	21.2 (5.0)	21.9 (6.7)

Notes. Data are presented as mean ± SD in parentheses, unless otherwise indicated.

[a]There were missing data for the following variables: handedness (1 patient with schizophrenia) and parental social class (2 healthy volunteers and 1 patient with schizophrenia).

[b]Parental social class was coded from 1 (highest) to 5 (lowest) using the Hollingshead Redlich Scale (1958).

Table 2

Mean FA (x1000) Values for Patients and Healthy Volunteers [1]

	SZ N = 35	BP N = 20	HC N = 56	Adjusted Confidence Intervals of Difference Between Groups [2]					
				HC - SZ		HC - BP		SZ - BP	
	Mean (SD)	Mean (SD)	Mean (SD)	95% CI	Effect Size	95% CI	Effect Size	95% CI	Effect Size
Frontal Lobe	281 (18.4)	282 (19.0)	279 (24.6)	−10.4 to 8.5	.000	−13.7 to 10.1	.001	−10.8 to 8.7	.001
Superior frontal gyrus	312 (16.3)	310 (20.9)	305 (30.5)	−16.6 to 5.3	.012	−18.5 to 10.4	.004	−8.3 to 11.1	.002
Middle frontal gyrus	278 (23.4)	278 (24.5)	274 (24.9)	−13.3 to 6.8	.005	−15.3 to 10.0	.002	−10.5 to 11.7	.000
Inferior frontal gyrus	256 (21.5)	264 (19.5)	258 (21.5)	−7.1 to 11.4	.002	−17.3 to 4.5	.018	−20.6 to 2.8	.042
Precentral gyrus	301 (17.5)	306 (21.5)	303 (20.6)	−4.3 to 11.4	.009	−11.4 to 8.4	.001	−16.0 to 5.2	.020
Middle orbitofrontal gyrus	288 (41.1)	278 (46.1)	286 (50.8)	−20.3 to 20.0	.000	−16.8 to 34.9	.007	−14.1 to 33.2	.012
Lateral orbitofrontal gyrus	250 (29.2)	253 (32.4)	248 (28.8)	−14.7 to 10.3	.001	−21.0 to 10.1	.007	−20.4 to 13.3	.003
Parietal Lobe	261 (15.9)	269 (15.0)	266 (20.3)	−2.9 to 13.1	.018	−12.6 to 7.1	.004	−16.8 to 0.7	.061
Postcentral gyrus	288 (15.5)	288 (18.9)	289 (20.1)	−6.7 to 9.1	.001	−8.1 to 12.0	.002	−9.0 to 9.7	.000
Superior parietal gyrus	276 (21.0)	288 (18.3)	283 (27.1)	−2.7 to 18.6	.024	−16.9 to 9.1	.005	−23.3 to −0.7	.080[a]
Supramarginal gyrus	236 (25.3)	247 (23.8)	241 (24.6)	−6.0 to 15.4	.009	−19.3 to 6.2	.014	−25.3 to 2.8	.047
Angular gyrus	257 (25.1)	270 (23.3)	265 (24.3)	−2.5 to 18.6	.025	−17.1 to 7.7	.008	−26.8 to 0.9	.064
Precuneus	249 (22.7)	253 (19.4)	252 (23.6)	−6.3 to 13.6	.006	−12.4 to 11.0	.000	−16.4 to 7.6	.010
Limbic Lobe	273 (14.6)	279 (15.4)	280 (20.7)	−1.1 to 15.0	.033	−9.0 to 11.3	.001	−14.3 to 2.5	.037
Cingulate gyrus	275 (30.8)	282 (24.5)	285 (28.8)	−2.8 to 22.8	.027	−11.4 to 17.6	.003	−23.4 to 9.2	.015
Hippocampus	272 (21.9)	276 (25.1)	276 (27.1)	−7.0 to 14.8	.006	−14.7 to 13.1	.000	−17.6 to 8.3	.010
Occipital Lobe	236 (15.4)	258 (21.0)	252 (26.4)	7.1 to 26.7	.117[d]	−18.4 to 7.8	.009	−32.1 to −12.5	.287[d]
Superior occipital gyrus	240 (29.0)	266 (25.3)	262 (40.5)	6.6 to 38.1	.083[b]	−23.6 to 15.3	.002	−42.2 to −10.7	.179[d]
Middle occipital gyrus	238 (17.0)	258 (22.2)	254 (21.7)	7.6 to 24.8	.138[d]	−15.2 to 7.3	.007	−31.1 to −9.8	.221[d]
Inferior occipital gyrus	229 (22.0)	249 (35.0)	241 (34.0)	−0.6 to 25.0	.039	−25.6 to 10.0	.010	−34.9 to −5.2	.123[b]
Temporal Lobe	244 (12.9)	258 (18.1)	251 (21.0)	−0.2 to 15.6	.041	−17.3 to 4.0	.021	−22.9 to −6.0	.184[d]
Superior temporal gyrus	226 (16.1)	236 (12.6)	235 (17.0)	2.2 to 16.5	.072[a]	−8.5 to 8.0	.000	−18.3 to −1.4	.095[a]
Middle temporal gyrus	270 (19.8)	279 (14.9)	275 (18.9)	−2.7 to 13.7	.020	−13.5 to 5.1	.011	−20.0 to 0.5	.065
Inferior temporal gyrus	242 (16.2)	256 (25.9)	251 (23.4)	1.3 to 19.1	.056[a]	−16.5 to 8.4	.006	−25.8 to −2.8	.107[a]

	SZ N = 35	BP N = 20	HC N = 56	Adjusted Confidence Intervals of Difference Between Groups [2]					
				HC - SZ		HC - BP		SZ - BP	
	Mean (SD)	Mean (SD)	Mean (SD)	95% CI	Effect Size	95% CI	Effect Size	95% CI	Effect Size
Parahippocampal gyrus	225 (22.6)	247 (23.4)	237 (28.7)	0.0 to 22.8	.043[a]	−25.3 to 3.2	.032	−35.2 to −9.3	.186[d]
Fusiform gyrus	256 (29.4)	272 (37.9)	259 (43.1)	−14.4 to 18.8	.001	−35.6 to 8.2	.021	−34.5 to 2.5	.055

[a] $p \leq .05$

[b] $p \leq .01$

[c] $p \leq .005$

[d] $p \leq .001$

[1] Analyses presented for descriptive purposes only;

[2] Adjusted for age

Table 3

Mean Diffusivity in $(\mu m)^2/s$ Values in Gray Matter for Patients and Healthy Volunteers [1]

				Adjusted Confidence Intervals of Difference Between Groups [2]					
	SZ N = 35	BP N = 20	HC N = 56	HC - SZ		HC - BP		SZ - BP	
	Mean (SD)	Mean (SD)	Mean (SD)	95% CI	Effect Size	95% CI	Effect Size	95% CI	Effect Size
Frontal Lobe	1199 (65.1)	1230 (71.8)	1184 (66.0)	−45.0 to 7.0	.023	−82.4 to −16.7	.110[a]	−63.4 to 3.2	.060
Superior frontal gyrus	1175 (79.6)	1221 (88.4)	1184 (77.1)	−27.1 to 35.6	.001	−81.2 to −3.4	.060[a]	−88.3 to −3.0	.082[a]
Middle frontal gyrus	1220 (68.0)	1265 (74.6)	1223 (76.6)	−30.4 to 28.2	.000	−82.7 to −10.2	.082[a]	−81.5 to −7.1	.099[a]
Inferior frontal gyrus	1229 (64.2)	1252 (55.3)	1205 (56.2)	−50.2 to −2.5	.052[a]	−76.8 to −19.9	.136[d]	−51.9 to 6.5	.045
Precentral gyrus	1258 (81.5)	1316 (95.0)	1249 (93.5)	−49.2 to 21.7	.007	−116.9 to −26.4	.12[c]	−102.3 to −11.5	.109[a]
Middle orbitofrontal gyrus	1064 (103.0)	1078 (116.7)	1049 (101.2)	−60.9 to 25.8	.007	−86.9 to 21.3	.020	−71.5 to 43.2	.005
Lateral orbitofrontal gyrus	1250 (82.1)	1247 (93.7)	1194 (91.4)	−95.5 to−23.5	.109[d]	−103.0 to −8.5	.070[a]	−41.7 to 47.6	.000
Parietal Lobe	1297 (88.1)	1314 (69.1)	1265 (101.5)	−75.7 to 0.8	.041	−100.0 to −10.1	.075[a]	−59.5 to 25.7	.012
Postcentral gyrus	1298 (93.4)	1338 (87.1)	1269 (107.0)	−75.2 to 5.3	.033	−123.3 to −26.7	.116[c]	−86.3 to 8.5	.050
Superior parietal gyrus	1387 (138.4)	1404 (110.0)	1345 (158.7)	−109.7 to 8.8	.031	−137.1 to −0.3	.052[a]	−84.6 to 51.9	.004
Supramarginal gyrus	1240 (60.8)	1257 (57.4)	1208 (86.5)	−67.8 to −3.6	.053[a]	−93.2 to −12.4	.085[a]	−48.3 to 14.6	.022
Angular gyrus	1249 (78.3)	1243 (58.8)	1205 (85.4)	−81.5 to −13.7	.081[b]	−81.1 to −1.5	.055[a]	−32.2 to 44.9	.002
Precuneus	1311 (93.0)	1330 (62.3)	1298 (103.3)	−57.9 to 21.2	.010	−83.3 to 8.4	.035	−62.3 to 24.6	.014
Limbic Lobe	1228 (50.1)	1225 (47.7)	1195 (45.8)	−54.4 to −14.7	.120[d]	−55.2 to −7.7	.087[b]	−24.5 to 30.4	.001
Cingulate gyrus	1165 (47.2)	1181 (49.4)	1156 (54.4)	−31.8 to 10.8	.011	−53.9 to −0.9	.055[a]	−41.4 to 8.5	.032
Hippocampus	1292 (72.0)	1270 (75.4)	1234 (59.1)	−86.2 to −31.1	.169[d]	−68.9 to −2.1	.058[a]	−19.2 to 64.0	.022
Occipital Lobe	1225 (81.5)	1203 (68.3)	1195 (71.6)	−64.0 to −2.7	.050[a]	−46.4 to 23.6	.006	−19.1 to 63.3	.022
Superior occipital gyrus	1348 (131.2)	1318 (113.7)	1299 (106.4)	−102.1 to −7.1	.056[a]	−77.5 to 28.5	.011	−37.0 to 98.8	.016
Middle occipital gyrus	1175 (79.5)	1147 (57.3)	1140 (63.3)	−66.9 to −8.6	.070[a]	−40.3 to 22.5	.004	−11.1 to 68.4	.039
Inferior occipital gyrus	1151 (69.9)	1145 (80.5)	1147 (87.3)	−41.6 to 26.2	.002	−44.7 to 43.2	.000	−33.2 to 46.8	.002
Temporal Lobe	1128 (50.5)	1121 (44.7)	1091 (46.6)	−59.2 to −19.2	.147[d]	−55.6 to −7.9	.088[b]	−19.8 to 33.7	.005
Superior temporal gyrus	1219 (58.7)	1231 (61.4)	1188 (52.4)	−56.7 to −11.7	.094[c]	−73.7 to −18.0	.128[c]	−44.1 to 20.3	.010

				Adjusted Confidence Intervals of Difference Between Groups [2]					
	SZ N = 35	BP N = 20	HC N = 56	HC - SZ		HC - BP		SZ - BP	
	Mean (SD)	Mean (SD)	Mean (SD)	95% CI	Effect Size	95% CI	Effect Size	95% CI	Effect Size
Middle temporal gyrus	1092 (47.7)	1067 (50.7)	1057 (62.7)	−61.5 to −13.0	.096[c]	−42.9 to 19.1	.008	−2.4 to 52.4	.061
Inferior temporal gyrus	968 (83.4)	929 (48.0)	914 (75.1)	−89.2 to −22.6	.112[d]	−51.8 to 20.5	.010	−1.4 to 80.1	.067
Parahippocampal gyrus	1250 (70.1)	1263 (69.9)	1,210 (59.6)	−69.2 to −15.7	.101[c]	−87.0 to −22.2	.134[d]	−52.2 to 26.4	.008
Fusiform gyrus	1112 (49.7)	1116 (51.2)	1086 (47.4)	−46.9 to −5.6	.068[a]	−56.0 to −5.4	.074[a]	−32.9 to 23.3	.002

[a] $p \leq .05$

[b] $p \leq .01$

[c] $p \leq .005$

[d] $p \leq .001$

[1] Analyses presented for descriptive purposes only;

[2] Adjusted for age